

文章编号: 1006-6616 (2012) 02-0178-09

西藏冈底斯东段南缘桑布加拉辉钼矿 Re-Os 定年及地质意义

赵 珍¹, 胡道功¹, 吴珍汉², 陆 露²

(1. 中国地质科学院地质力学研究所, 北京 100081;

2. 中国地质科学院, 北京 100037)

摘要: 雅鲁藏布江缝合带北侧的桑布加拉矽卡岩型铜矿床为冈底斯成矿带南亚带典型多金属矿床之一。该矿床的8件辉钼矿样品Re-Os等时线年龄为(93.3 ± 4.1) Ma, 平均模式年龄为(94.5 ± 1.6) Ma, 表明桑布加拉矿床形成于晚白垩世新特提斯洋向北俯冲消减阶段。洋壳俯冲消减阶段形成的桑布加拉铜矿床及其新生代不同时期多金属矿床的发现, 说明冈底斯成矿带在俯冲消减阶段、主碰撞阶段、晚碰撞阶段和后碰撞阶段均存在大规模成矿作用, 并构成完整的成矿演化系列。

关键词: Re-Os 同位素年龄; 辉钼矿; 矽卡岩型铜矿; 冈底斯; 成矿演化

中图分类号: P597

文献标识码: A

0 引言

冈底斯成矿带是一条资源潜力巨大的铜多金属成矿带, 可进一步分为3个亚带, 即北部勒青拉—洞中松多热液脉型、矽卡岩型银铅锌多金属矿带, 中部厅宫—驱龙斑岩型铜钼铅锌矿带和南部克鲁—冲木达矽卡岩型、斑岩型铜金矿带^[1]。

近年来, 冈底斯成矿带的研究工作取得了诸多成果和重要进展, 划分出印-亚大陆碰撞前的俯冲成矿阶段(距今180~65 Ma)、主碰撞造山成矿阶段(距今65~41 Ma)、晚碰撞转换成矿阶段(距今40~26 Ma)以及后碰撞伸展成矿阶段(距今25~0 Ma)等重要成矿期^[2]。对成岩成矿时代的研究也日趋深入, 获得了大量可靠的数据, 其中北亚带成矿时代在距今50~65 Ma之间, 中亚带集中在距今14~17 Ma, 而南亚带成矿时代较为分散, 仍存在较大争议^[3~5]。本文对南亚带桑布加拉铜矿进行成矿时代的测定, 不仅可以深入研究南亚带的成矿机制, 同时为研究冈底斯成矿带各亚带的时空关系、冈底斯成矿带与板块俯冲—碰撞构造岩浆活动有关的成矿演化过程提供有力的支持。

1 构造岩浆成矿背景

冈底斯成矿带位于拉萨地体南缘雅鲁藏布江缝合带北侧, 东西长约2000 km, 南北宽约

收稿日期: 2011-12-08

基金项目: 中国地质调查局项目(编号: 1212011120185)

作者简介: 赵珍(1987-), 女, 硕士研究生, 构造地质学专业。E-mail: zhaozhen03@126.com

100 km (见图1)。在特提斯构造演化过程中, 经历了石炭纪—三叠纪活动大陆边缘、侏罗纪—早白垩世特提斯多岛弧盆系统、白垩纪末—始新世亚欧-印度大陆碰撞造山和中新世以来后碰撞伸展等多个构造演化阶段^[16~18]。

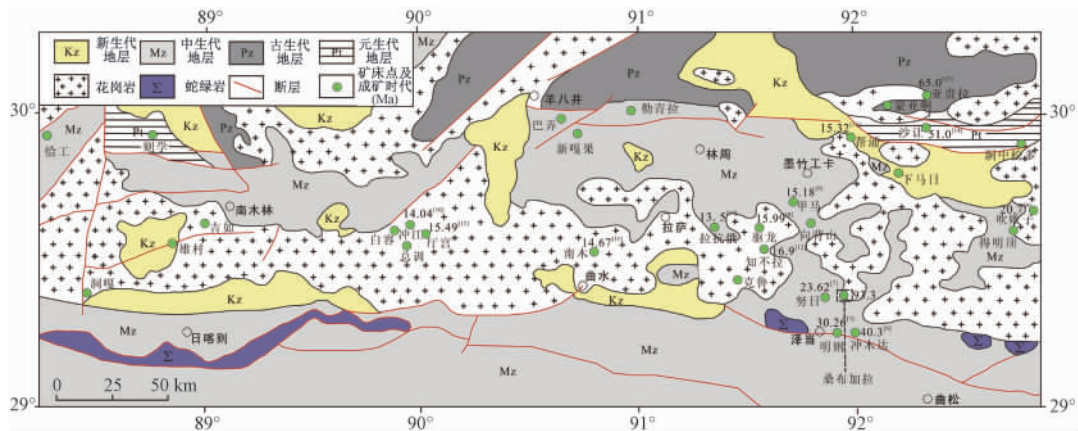


图1 冈底斯矿带地质简图及矿床分布 (据文献[3]修改)

Fig. 1 Simplified geological map of the Gangdese ore belt and distribution of deposits

冈底斯带岩浆活动从白垩纪持续到第三纪, 侵位高峰为距今 55~45 Ma 和距今 30~24 Ma^[19~20], 广泛分布燕山晚期至喜马拉雅期的中酸性火山岩和岩浆岩, 构成了冈底斯火山-岩浆杂岩带。火山岩以燕山期为主, 为中酸性安山质一流纹质火山熔岩及火山碎屑岩, 具活动大陆边缘火山岩特征; 喜马拉雅期火山活动为陆相火山喷发, 以钙碱性火山岩为主; 晚期偏碱性, 具岛弧火山岩特征。侵入岩多呈带状分布的复式岩基、岩株和岩脉, 燕山晚期(距今 110~75 Ma)以中酸性岩为主, 后期出现偏碱性花岗岩, 多属Ⅰ型花岗岩类。燕山期花岗岩多形成大的岩基, 构成花岗岩带的主体; 喜马拉雅期花岗岩多呈小的岩体、岩株, 与该带成矿作用密切相关^[21]。

火山-岩浆弧演化过程不仅能够反映板块运动过程中俯冲与碰撞作用的时空对应关系, 也伴随对应的成矿事件^[22]。冈底斯带岩浆活动的两个高峰期分别对应亚欧-印度大陆大规模碰撞(距今 55~50 Ma)^[23~24]和冈底斯逆冲断裂活动(距今 20~30 Ma)^[25~26]。晚古生代活动大陆边缘的当雄—工布江达一带, 发育有伸展环境的双峰式火山活动和裂谷盆地沉积组合, 形成了北亚带矿床系列; 中生代多岛弧盆系的冈底斯南缘, 由于弧火山和深成侵入活动, 发育钙碱性岛弧-陆缘弧花岗岩, 形成了南亚带矿床系列; 距今 21 Ma 左右, 冈底斯造山带快速隆升, 随后发生东西向伸展, 产生近南北向的裂谷, 与此对应, 冈底斯带发育钾玄质-高钾钙碱性熔岩^[27]、规模较小的高位花岗岩体和花岗质斑岩体, 形成了中亚带矿床系列^[28]。

2 矿床地质特征

桑布加拉矿床地层主要为白垩系桑日群比马组泥晶灰岩、变质粉砂岩以及白垩系花岗闪长岩, 地层主体呈近东西向展布。其中花岗闪长岩侵入到比马组中, 发生热液接触交代作用, 为岩浆热液接触交代矽卡岩型铜矿(见图2、图3a)。矿体主要产在与泥灰岩接触的矽卡岩中, 呈不规则长条-透镜状, 近北东-东西走向, 出露面积小于 0.2 km²。赋矿岩石为

灰绿色、灰白色石榴子石矽卡岩，团块状、浸染状构造，细粒、变晶粒状结构；矿石矿物有黄铜矿、黄铁矿、斑铜矿、辉钼矿、铜蓝等，呈细脉状、浸染状、星簇状分布（见图3b—3d）。显微特征如图3e，金属矿物生成顺序为：磁铁矿→赤铁矿→黄铁矿→磁黄铁矿→黄铜矿→铜蓝→褐铁矿；脉石矿物有石英、长石、透辉石、硅灰石等；Cu矿石品位0.40%~6.84%，平均3.47%^[28]。

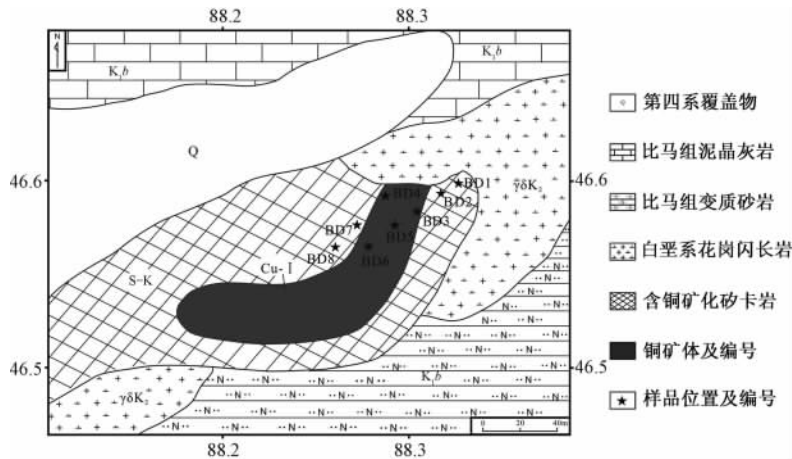


图2 桑布加拉矿区地质简图

Fig. 2 Simple geological map of Sangbujiala copper deposit

在矿区采剖面东部可见闪长岩与矽卡岩的接触关系（见图3f），向西矿化逐渐增强，以泥灰岩处蚀变最为强烈，发育大量黄铜矿、黄铁矿。采剖面下部，可见小型花岗闪长岩株。区内发育大量南北向、北东东向、北西西向的节理、裂隙，并被后期部分含矿的石英脉、方解石脉充填，其中石英脉里以黄铜矿化为主，方解石脉里以黄铁矿化为主。方解石脉被后期石英脉切穿。根据脉体、裂隙等的先后切割关系，划分以下成矿期次：早期为主成矿期的接触蚀变作用矽卡岩成矿，晚期为破裂面内方解石脉成矿，更晚期为石英脉成矿。

为了获得可靠的成矿时代，在该矿区采集了与矿化密切相关的8件含辉钼矿的矽卡岩样品，进行辉钼矿Re-Os同位素测试（样品位置见图2），样品均采自接触蚀变作用形成的主成矿期矽卡岩。辉钼矿呈星簇状、浸染状、细脉状分布。辉钼矿显微特征如图3g，呈鳞片状，片直径0.1~0.2 mm，部分0.2~0.5 mm，反射色为灰白色、灰色，不透明矿物生成顺序：辉钼矿→磁铁矿→赤铁矿。

3 测试结果

同位素年龄测试在国家地质实验测试中心铼-锇同位素实验室完成，Re-Os同位素分析结果见表1。辉钼矿Re含量变化较大，其中样品BD4 Re含量明显较其他样品低，但是不影响测试结果，Re/¹⁸⁷Os值较一致，模式年龄从(92.13±1.26) Ma到(97.62±1.62) Ma。采用Isoplot软件作等时线和加权平均值，得到等时线年龄为(93.3±4.1) Ma，初始¹⁸⁷Os为(1±3) ng/g（见图4），平均模式年龄为(94.5±1.6) Ma（见图5），与等时线年龄相差1.3~4.5 Ma。

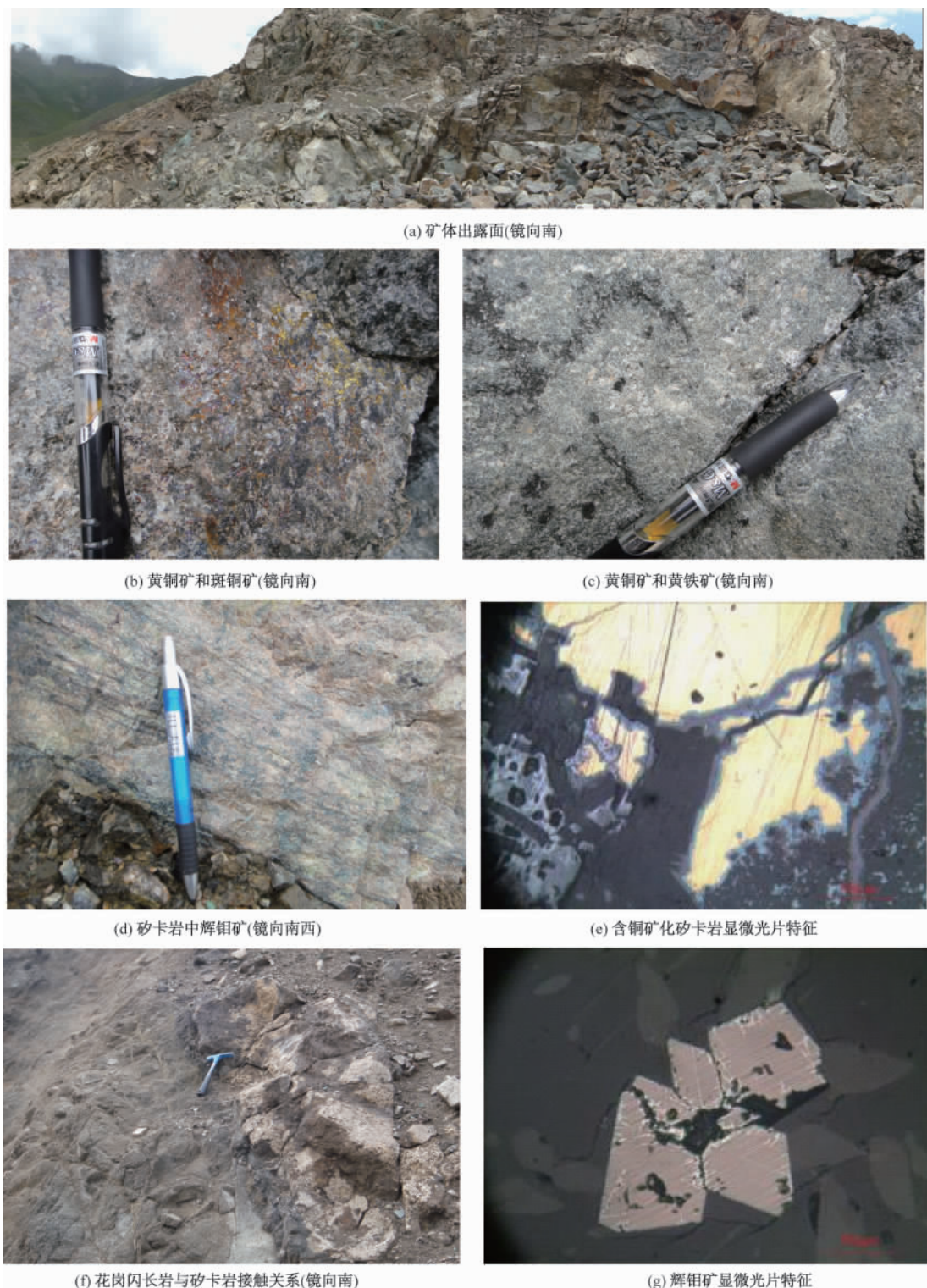


图3 桑布加拉矿区野外照片

Fig. 3 Photos of Sangbujiala copper deposit

表1 桑布加拉铜矿辉钼矿 Re-Os 同位素数据

Table 1 Re-Os isotopic datum of molybdenite from Sangbujiala copper deposit

| 样品号 | 样品重量/g | $\text{Re}/(\mu\text{g} \cdot \text{g}^{-1})$ | $\text{普 Os}/(\text{ng} \cdot \text{g}^{-1})$ | $^{187}\text{Re}/(\mu\text{g} \cdot \text{g}^{-1})$ | $^{187}\text{Os}/(\text{ng} \cdot \text{g}^{-1})$ | 模式年龄/Ma |
|-----|---------|---|---|---|---|------------------|
| BD1 | 0.03023 | 65.97 ± 0.67 | 0.1885 ± 0.0339 | 41.47 ± 0.42 | 67.49 ± 0.69 | 97.62 ± 1.62 |
| BD2 | 0.02062 | 104.6 ± 0.8 | 0.0003 ± 0.0290 | 65.73 ± 0.49 | 101.2 ± 0.8 | 92.31 ± 1.26 |
| BD3 | 0.01188 | 82.59 ± 0.62 | 0.0136 ± 0.0608 | 51.91 ± 0.39 | 82.97 ± 0.76 | 95.87 ± 1.38 |
| BD4 | 0.05094 | 8.604 ± 0.066 | 0.8471 ± 0.0078 | 5.408 ± 0.042 | 8.31 ± 0.07 | 92.13 ± 1.26 |
| BD5 | 0.03064 | 87.36 ± 0.67 | 0.1414 ± 0.0204 | 54.90 ± 0.42 | 85.81 ± 0.68 | 93.74 ± 1.28 |
| BD6 | 0.03068 | 56.06 ± 0.43 | 1.969 ± 0.033 | 35.23 ± 0.27 | 55.63 ± 0.44 | 94.69 ± 1.29 |
| BD7 | 0.03048 | 45.85 ± 0.41 | 0.0551 ± 0.0140 | 28.82 ± 0.26 | 46.05 ± 0.42 | 95.85 ± 1.45 |
| BD8 | 0.03097 | 62.47 ± 0.63 | 6.095 ± 0.058 | 39.27 ± 0.40 | 62.81 ± 0.51 | 95.95 ± 1.47 |

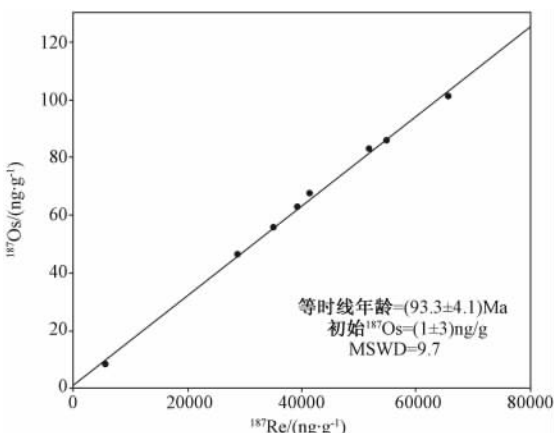


图4 桑布加拉铜矿辉钼矿 Re-Os 同位素等时线

Fig. 4 Re-Os isotope line of molybdenite from Sangbujiala copper deposit

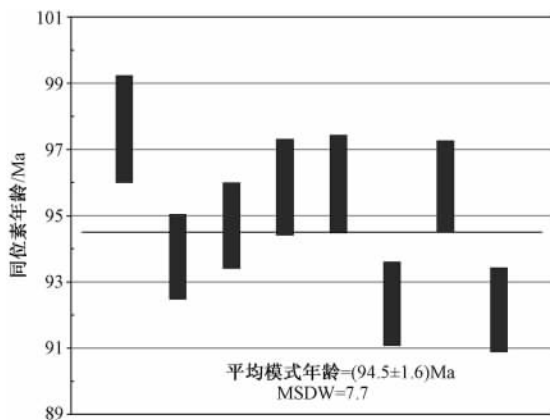


图5 桑布加拉铜矿辉钼矿 Re-Os 平均模式年龄

Fig. 5 The average of Re-Os model age of molybdenite from Sangbujiala copper deposit

4 讨论与结论

此次辉钼矿样品采自与矿体同生的矽卡岩中，因此辉钼矿 Re-Os 等时线的年龄能够代表成矿年龄，即桑布加拉矿床的成矿年龄是 (93.3 ± 4.1) Ma，为燕山晚期晚白垩世，早于大陆碰撞时代，是俯冲阶段成矿。梁华英等^[29]对桑布加拉矿化岩体石英二长岩进行锆石 (LA-ICPMS) U-Pb 测定，获得年龄为 (92.1 ± 0.6) Ma，与本次辉钼矿 Re-Os 等时线年龄 (93.3 ± 4.1) Ma 一致。

陈毓川等^[30]提出，一个成矿省无论空间范围大小、演化历史长短，其成矿系列中都应具有不同地质演化阶段形成的各种成矿作用。因此，青藏高原从特提斯洋俯冲到印-亚大陆碰撞-伸展的整个岩浆-构造演化，也应该有比较完整的矿床系列。

大量测试结果表明，南亚带成矿时代在距今 $20 \sim 40$ Ma 之间，如：明则矿床 (30.26 ± 0.69) Ma^[7]、努日矿床 (23.62 ± 0.97) Ma^[7]，主要是晚碰撞转换阶段成矿；中亚带成矿时代集中在距今 $14 \sim 17$ Ma，如：驱龙矿床 (15.99 ± 0.32) Ma^[8]、甲马矿床 (15.18 ± 0.98) Ma^[9]，为后碰撞伸展阶段成矿；北亚带成矿时代在距今 $50 \sim 65$ Ma 之间，如：沙

让矿床 (51.0 ± 1.0) Ma^[14]、亚贵拉矿床 (65.0 ± 1.9) Ma^[15]，主要是主碰撞造山阶段成矿。而本次获得的桑布加拉矿床成矿时代 (93.3 ± 4.1) Ma 明显早于冈底斯东段已知的成矿时代，并且在构造岩浆演化上早于碰撞造山阶段成矿，属于新特提斯洋壳向北俯冲消减阶段成矿（见图 1、图 6）。



图 6 冈底斯东段多期成矿事件年代学简图（据文献 [1] 修改）

Fig. 6 Chronology of metallogenic stages in eastern Gangdese

因此，此次获得的桑布加拉矿床的成矿时代，不仅说明冈底斯东段南缘存在碰撞前的洋壳俯冲阶段成矿，也说明冈底斯带构造岩浆与成矿事件是对应完整的演化序列。这对于重新认识冈底斯东段南缘矿带、拓宽找矿方向和范围、研究成矿规律和成矿作用具有重要意义。

致谢：野外工作得到西藏地质局第二地质大队巴登珠总工的指导与支持，特此致谢。

参 考 文 献

- [1] 范新, 陈雷, 秦克章, 等. 西藏山南地区明则斑岩钼矿蚀变矿化特征与成矿时代 [J]. 地质与勘探, 2011, 47 (1): 89~99.
FAN Xin, CHEN Lei, QIN Ke-zhang, et al. Characteristics of alteration and mineralization and chronology of the Mingze porphyry Mo deposit in the Shannan area of southern Tibet [J]. Geology and Exploration, 2011, 47 (1): 89~99.
- [2] 侯增谦, 潘桂棠, 王安建, 等. 青藏高原碰撞造山带: II. 晚碰撞转换成矿作用 [J]. 矿床地质, 2006, 25 (5): 521~543.
HOU Zeng-qian, PAN Gui-tang, WANG An-jian, et al. Metallogenesis in Tibetan collisional orogenic belt: II. Mineralization in late-collisional transformation setting [J]. Mineral Deposits, 2006, 25 (5): 521~543.
- [3] 余宏全, 丰成友, 张德全, 等. 西藏冈底斯中东段矽卡岩铜—铅—锌多金属矿床特征及成矿远景分析 [J]. 矿床地质, 2005, 24 (5): 508~520.
SHE Hong-quan, FENG Cheng-you, ZHANG De-quan, et al. Characteristics and metallogenetic potential of skarn copper-lead-zinc polymetallic deposits in central eastern Gangdese [J]. Mineral Deposits, 2005, 24 (5): 508~520.
- [4] 侯增谦, 杨竹森, 徐文艺, 等. 青藏高原碰撞造山带: I. 主碰撞造山成矿作用 [J]. 矿床地质, 2006, 25 (4): 337~358.
HOU Zeng-qian, YANG Zhu-sen, XU Wen-yi, et al. Metallogenesis in Tibetan collisional orogenic belt: I. Mineralization in main collisional orogenic setting [J]. Mineral Deposits, 2006, 25 (4): 337~358.
- [5] 芮宗瑶, 侯增谦, 李光明, 等. 冈底斯斑岩铜矿成矿模式 [J]. 地质论评, 2006, 52 (4): 459~466.
RUI Zong-yao, HOU Zeng-qian, LI Guang-ming, et al. A genetic model for the Gandise porphyry copper deposits [J]. Geological Review, 2006, 52 (4): 459~466.
- [6] 李光明, 刘波, 余宏全, 等. 西藏冈底斯成矿带南缘喜马拉雅早期成矿作用——来自冲木达铜金矿床的 Re-Os 同位素年龄证据 [J]. 地质通报, 2006, 25 (12): 1482~1486.

- LI Guang-ming, LIU Bo, SHE Hong-quan, et al. Early Himalayan mineralization on the southern margin of the Gangdise metallogenic belt, Tibet, China: Evidence from Re-Os ages of the Chongmuda skarn-type Cu-Au deposit [J]. Geological bulletin of China, 2006, 25 (12): 1482 ~ 1486.
- [7] 闫学义, 黄树峰, 杜安道. 冈底斯泽当大型钨铜钼矿 Re-Os 年龄及陆缘走滑转换成矿作用 [J]. 地质学报, 2010, 84 (3): 398 ~ 406.
- YAN Xue-yi, HUANG Shu-feng, DU An-dao. Re-Os ages of large tungsten, copper and molybdenum deposit in the Zetang orefield, Gangdise and marginal strike-slip transforming metallogenesis [J]. Acta Geological Sinica, 2010, 84 (3): 398 ~ 406.
- [8] 芮宗瑶, 侯增谦, 曲晓明, 等. 冈底斯斑岩铜矿成矿时代及青藏高原隆升 [J]. 矿床地质, 2003, 22 (3): 217 ~ 225.
- RUI Zong-yao, HOU Zeng-qian, QU Xiao-ming, et al. Metallogenetic epoch of Gangdese porphyry copper belt and uplift of Qinghai-Tibet Plateau [J]. Mineral Deposits, 2003, 22 (3): 217 ~ 225.
- [9] 芮宗瑶, 李光明, 张立生, 等. 西藏斑岩铜矿对重大地质事件的响应 [J]. 地学前缘, 2004, 11 (1): 145 ~ 152.
- RUI Zong-yao, LI Guang-ming, ZHANG Li-sheng, et al. The response of porphyry copper deposits to important geological events in Xizang [J]. Earth Science Frontiers, 2004, 11 (1): 145 ~ 152.
- [10] 侯增谦, 曲晓明, 王淑贤, 等. 西藏高原冈底斯斑岩铜矿带辉钼矿 Re-Os 年龄: 成矿作用时限与动力学背景应用 [J]. 中国科学: D 辑, 2003, 33 (7): 609 ~ 618.
- HOU Zeng-qian, QU Xiao-ming, WANG Shu-xian, et al. Re-Os age for molybdenite from the Gangdese porphyry copper belt on Tibetan plateau: Duration of the Cu mineralization for geodynamic setting [J]. Science in China: Series D, 2003, 33 (7): 609 ~ 618.
- [11] 曲晓明, 侯增谦, 黄卫. 冈底斯斑岩铜矿(化)带: 西藏第二个“玉龙”铜矿带? [J]. 矿床地质, 2001, 20 (4): 355 ~ 366.
- QU Xiao-ming, HOU Zeng-qian, HUANG Wei. Is Gangdese porphyry copper belt the second “Yulong” copper belt? [J]. Mineral Deposits, 2001, 20 (4): 355 ~ 366.
- [12] 李光明, 刘波, 屈文俊, 等. 西藏冈底斯成矿带的斑岩—矽卡岩成矿系统: 来自斑岩矿床和矽卡岩型铜多金属矿床的 Re-Os 同位素年证据 [J]. 大地构造与成矿学, 2005, 29 (4): 482 ~ 490.
- LI Guang-ming, LIU Bo, QU Wen-jun, et al. The porphyry-skarn ore-forming system in Gangdese metallogenic belt, southern Xizang: Evidence from molybdenite Re-Os age of porphyry-type copper deposits and skarn-type copper polymetallic deposits [J]. Geotectonica et Metallogenesis, 2005, 29 (4): 482 ~ 490.
- [13] 孟祥金, 侯增谦, 高永丰, 等. 西藏冈底斯东段斑岩铜钼铅锌成矿系统的发育时限: 帮浦铜多金属矿床辉钼矿 Re-Os 年龄证据 [J]. 矿床地质, 2003, 22 (3): 246 ~ 252.
- MENG Xiang-jin, HOU Zeng-qian, GAO Yong-feng, et al. Development of porphyry copper-molybdenum lead-Zinc ore-forming system in east Gangdese belt, Tibet: Evidence from Re-Os age of molybdenite in Bangpu copper polymetallic deposit [J]. Mineral Deposits, 2003, 22 (3): 246 ~ 252.
- [14] 唐菊兴, 陈毓川, 王登红, 等. 西藏工布江达县沙让斑岩钼矿床辉钼矿铼—锇同位素年龄及其地质意义 [J]. 地质学报, 2009, 83 (5): 698 ~ 704.
- TANG Ju-xing, CHEN Yu-chuan, WANG Deng-hong, et al. Re-Os dating of molybdenite from the Sharang porphyry molybdenum deposit in Gongbogyamda County, Tibet and its geological significance [J]. Acta Geological Sinica, 2009, 83 (5): 698 ~ 704.
- [15] 高一鸣, 陈毓川, 唐菊兴, 等. 西藏工布江达地区亚贵拉铅锌钼矿床辉钼矿 Re-Os 测年及其地质意义 [J]. 地质通报, 2011, 30 (7): 1027 ~ 1036.
- GAO Yi-ming, CHEN Yu-chuan, TANG Ju-xing, et al. Re-Os dating of molybdenite from the Yaguila porphyry molybdenum deposit in Gongbogyamda area, Tibet, and its geological significance [J]. Geological Bulletin of China, 2011, 30 (7): 1027 ~ 1036.
- [16] 潘桂棠, 莫宣学, 侯增谦, 等. 冈底斯造山带的时空结构及演化 [J]. 岩石学报, 2006, 22 (3): 521 ~ 533.
- PAN Gui-tang, MO Xuan-xue, HOU Zeng-qian, et al. Spatial-temporal framework of the Gangdese orogenic belt and its

- evolution [J]. *Acta Petrologica Sinica*, 2006, 22 (3): 521~533.
- [17] 李光明, 冯孝良, 黄志英. 西藏冈底斯构造带中段多岛弧盆系及其演化 [J]. 沉积与特提斯地质, 2000, 20 (4): 38~46.
LI Guang-ming, FENG Xiao-liang, HUANG Zhi-ying. The multiple island arc-basin systems and their evolution in the Gangdise tectonic belt, Xizang [J]. *Sedimentary Geology and Tethyan Geology*, 2000, 20 (4): 38~46.
- [18] 侯增谦, 莫宣学, 杨志明. 青藏高原碰撞造山带成矿作用: 构造背景、时空分布和主要类型 [J]. 中国地质, 2006, 33 (2): 348~359.
HOU Zeng-qian, MO Xuan-xue, YANG Zhi-ming, et al. Metallogens in the collisional orogen of the Qinghai-Tibet Plateau: Tectonic setting, tempo-spatial distribution and ore deposit types [J]. *Geology in China*, 2006, 33 (2): 348~359.
- [19] Schares E, Xu R H, Allegre C J. U-Pb geochronology of the Gangdese (Transhimalaya) plutonism in the Lhasa-Xizang region, Tibet [J]. *Earth and Planetary Science Letters*, 1984, 69: 311~320.
- [20] Harrison T M, Grove M, McKeegan K D, et al. Origin and episodic emplacement of the Manaslu intrusive complex, central Hiamalaya [J]. *Journal of Petrology*, 1999, 40 (1): 3~19.
- [21] 程力军, 李志, 刘鸿飞, 等. 冈底斯东段铜多金属成矿带的基本特征 [J]. 西藏地质, 2001, 19 (1): 43~53.
CHENG Li-jun, LI Zhi, LIU Hong-fei, et al. Basic features of the east Gangdise polymetallic metallogenic belt [J]. *Tibet Geology*, 2001, 19 (1): 43~53.
- [22] 王全海, 王保生, 李金高, 等. 西藏冈底斯岛弧及其铜多金属矿带的基本特征与远景评估 [J]. 地质通报, 2002, 21 (1): 35~40.
WANG Quan-hai, WANG Bao-sheng, LI Jin-gao, et al. Basic features and ore prospect evaluation of the Gangdise island arc, Tibet, and its copper polymetallic ore belt [J]. *Geological Bulletin of China*, 2002, 21 (1): 35~40.
- [23] Beck R A, Burbank D W, Sercombe W J, et al. Stratigraphic evidence for an early collision between northwest India and Asia [J]. *Nature*, 1995, 373: 55~58.
- [24] Le Fort P. Metamorphism and magmatism during the Himalayan collision [C] //Coward M P, Ries A C. Collision Tectonics. Oxford: Blackwell Scientific Publications, 1986: 159~172.
- [25] Yin A, Harrison T M, Ryerson F J, et al. Tertiary structural evolution of the Gangdese thrust system, southeastern Tibet [J]. *Journal of Geophysical Research*, 1994, 99 (B9): 18175~18201.
- [26] Yin A, Harrison T M. Geologic evolution of the Himalayan-Tibetan orogen [J]. *Annual Review of Earth and Planetary Sciences*, 2000, 28: 211~280.
- [27] Coulon C, Maluski H, Bollinger C, et al. Mesozoic and Cenozoic volcanic rocks from central and southern Tibet: $^{39}\text{Ar}/^{40}\text{Ar}$ dating, petrological characteristics and geodynamic significance [J]. *Earth and Planetary Science Letters*, 1986, 79 (3-4): 281~302.
- [28] 李光明, 王高明, 高大发. 西藏冈底斯南缘构造格架与成矿系统 [J]. 沉积与特提斯地质, 2002, 22 (2): 1~7.
LI Guang-ming, WANG Gao-ming, GAO Da-fa. The tectonic framework and metallogenic systems in southern Gangdise metallogenic belt, Xizang [J]. *Sedimentary Geology and Tethyan Geology*, 2002, 22 (2): 1~7.
- [29] 梁华英, 魏启荣, 许继峰, 等. 西藏冈底斯矿带南缘矽卡岩型铜矿床含矿岩体锆石 U-Pb 年龄及意义 [J]. 岩石学报, 2010, 26 (6): 1692~1698.
LIANG Hua-ying, WEI Qi-rong, XU Ji-feng, et al. Study on zircon LA-ICP-MS U-Pb age of skarn Cu mineralization related intrusion in the southern margin of the Gangdese ore belt, Tibet and its geological implication [J]. *Acta Petrologica Sinica*, 2010, 26 (6): 1692~1698.
- [30] 陈毓川, 王登红, 徐志刚, 等. 对中国成矿体系的初步探讨 [J]. 矿床地质, 2006, 25 (2): 155~163.
CHEN Yu-chuan, WANG Deng-hong, XU Zhi-gang, et al. Preliminary study of Chinese mineralization system [J]. *Mineral Deposits*, 2006, 25 (2): 155~163.

MOLYBDENITE Re-Os ISOTOPIC DATING OF SANGBUJIALA COPPER DEPOSIT IN THE SOUTH MARGIN OF THE EASTERN GANGDESE SECTION, TIBET, AND ITS GEOLOGICAL IMPLICATIONS

ZHAO Zhen¹, HU Dao-gong¹, WU Zhen-han², LU Lu²

(1. Institute of Geomechanics, Chinese Academy of Geological Sciences, Beijing 100081, China;

2. Chinese Academy of Geological Sciences, Beijing 100037, China)

Abstract: Located in north side of Yaluzangbujiang Suture, Sangbujiala skarn-type copper deposit is one of the typical polymetallic deposits in the south subzone of the Gangdese metallogenic belt. For the purpose of finding out the mineralization time, the authors selected eight molybdenite samples from Sangbujiala ore district to perform the Re-Os dating. The age of Re-Os isotime line from molybdenite is 93.3 ± 4.1 Ma, with an average model age of 94.5 ± 1.6 Ma. Therefore, the Sangbujiala ore formed during Late Cretaceous, which belongs to the Neo-Tethys subduction stage. The Sangbujiala ore and other Cenozoic deposits showed that the Gangdese metallogenic belt occurring large-scale mineralization in the subduction stage, main collision stage, late collision stage and post-collisional stage, and to form a complete series of metallogenic evolution.

Key words: Re-Os isotope age; molybdenite; skarn-type copper deposit; Gangdese; metallogenic evolution

(上接 109 页)

STUDY ON THE GEOMECHANICAL MODEL OF LANDSLIDE WITH LOW DIP ANGLE STRATA STRUCTURE: TAKING FENGDIAN LANDSLIDE AS AN EXAMPLE

WANG Zhi-hua, DU Ming-liang, GUO Zhao-cheng, JIA Wei-jie

(China Aero Geophysical Survey & Remote Sensing Center for Land and Resources, Beijing 100083, China)

Abstract: On the basis of research at home and abroad, starting from the landslide mechanism establish geomechanical model of landslides with low dip angle strata, all the parameters in the model, such as landslide size, slip angle, back edge ripping slot seepage depth and so on, were obtained by digital landslide technology and fields investigation and put them into the model formula then landslide critical friction coefficient can be obtained, and landslide total down-slide and total resistance slippery force shall be get. This is the first putting forward the concept of critical friction coefficient and calculating methods, and the coefficient directly related to the slippery ability or stability of the landslide. Analysis shows that the critical friction coefficient and landslide sliding body size (the length and width of the sliding surface), sliding plane obliquity are positive correlation, with landslide weight inversing relationship. The influence of the dip angle of the back wall changing in $60^\circ - 90^\circ$ on slippery ability of the landslide with low angle strata is very weak.

Key words: landslide with low-angled stratofabric structure; formation mechanism; geomechanical model; digital landslide technology; critical friction coefficient